Journal Name

COMMUNICATION

Expandable Porous Organic Frameworks with Built-In Amino and Hydroxyl Functions for CO_2 and CH_4 Capture

J. Perego, D. Piga, S. Bracco, P. Sozzani and A. Comotti*

Abstract. The synthesis of Porous Organic 3D Frameworks, wherein amine, hydroxyl and Li-alkoxide functions were built directly on the monomer-unit carbon core, realizes improved interactions with target gases. CO_2 was retained by the amine group with a remarkable energy of 54 kJ mol^{-1}, while 2D MAS NMR provided rare evidence of amine-to-gas short-distance interactions. Frameworks containing hydroxyl and Li-alkoxide functions show optimal interaction energy with CH_4 up to 25 kJ mol^{-1}. The light network of 3-branch building units ensures expandability of the nano-sponges.

Gas capture and storage is a prominent issue for our society, since it enables solutions for environmental and energy problems, especially for the target gases carbon dioxide and methane, both massively present in the atmosphere and in the lithosphere, and their connection to power and heat generation.[1] Porous materials can efficiently store a considerable amount of such gases with a moderate energy consumption for the gas release, thus ensuring a sound energy balance in sorption/release cycles.[2]

In recent years there has been an increasing number of porous materials obtained by exploiting the formation of a variety of interactions and chemical bonds, which span from soft interactions up to metal-organic and covalent bonds.[3] Among these families, porous organic frameworks (POFs) boast some prerogatives derived by the stability of their 3D network of covalent bonds. These prerogatives include the absence of potentially toxic metal ions, high thermal robustness, resistence to solvents, especially water, and remarkable volumetric and gravimetric pore capacity.[4] Further important properties are enabled by the post-synthetic insertion of organic functional-groups, each promoting specific interactions with target gases.[4] Thus, in the search for enhanced interactions by innovative solutions, we prepared new porous organic frameworks, starting from simple 3D synthons bearing organic functions. In our design, tetrahedral cores bear both the branches and the functional groups, which will be retained in the skeleton of the resulting framework. Therefore, the permanent motif of the frameworks is constituted by three *p*-phenylene rings protruding from a central core, a forth substituent being the chosen organic function directly bonded to the same core, yielding low-density architectures denominated Triphenylmethane Aromatic Frameworks (TAFs). By this synthetic strategy, the branches sustain the porous network and the functions protrude towards the empty spaces of the pores (Scheme 1). The functions are regularly bound onto the aliphatic carbon and do not modify the reactivity of the aromatic groups during the condensation reaction.

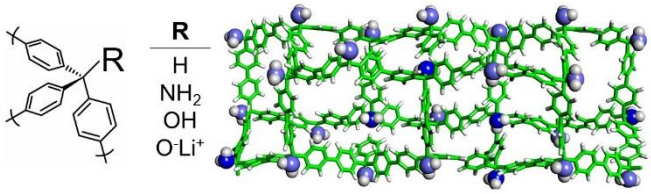

Scheme 1. Chemical structure of TAFs (above). Schematic representation of the porous organic polymer with walls decorated with –NH_2 groups (below).

The organic functions are exposed to the gases diffused into the framework. As a result, the behavior of the 3D frameworks with hydroxyl and aliphatic amine groups (TAF-OH and TAF-NH_2) is quite distinct from that of the fully hydrocarburic network (TAF): the amine functionalized compound exhibits an outstanding affinity for CO_2, while Li-alkoxide-containing framework (TAF-OLi) shows an enhanced affinity for CH_4. Solid state NMR provided unique evidence for close proximity of the gas to the walls, and the CO_2 interaction with the nanopore environment. The present work is part of the effort being spent for obtaining a gas affinity modulated by the wall nature and POF functionalization.

Monomers to be polymerized by Ni-catalysed Yamamoto coupling reaction require bromine atoms substituted on the aromatic rings in para-position. The presence of three such sacrificial functions on each monomer ensures a large number of cross-links, according to the Flory's polycondensation law, which dictates particle gelation will occur as soon as functional group conversion (p) overcomes the value of 0.66 ($DP_{n(inf.)}$= 2/(2-3p)).[5] However, reaction proceeds beyond this point, leading to less than 2-3% unreacted bromine substituents (ESI). Powder XRD revealed no short-range periodicity, as typically occurs in covalent frameworks obtained by irreversible bond formation (ESI). Solid state MAS NMR spectra of the powders recorded on ^{13}C and ^{1}H nuclei indicate the formation of carbon-carbon bonds between the aromatic rings and highlight the

[a] *Department of Materials Science, University of Milano Bicocca, Via R. Cozzi 55, 20125 Milan, Italy*

Electronic Supplementary Information (ESI) available: Synthesis and preparation of materials, PXRD, IR, TGA, solid state NMR, CO_2, CH_4 and N_2 adsorption isotherms.

dramatic change of tetrahedral carbon chemical shift due to the presence of hydrogen or organic-function substitution. The ^{13}C quantitative spectra evaluation confirm the full retention of -OH and -NH_2 substituents (1 per monomer unit) upon polymerization, as expected by Yamamoto coupling (Figure 1). This is an indication for optimal regularity in terms of constant stoichiometry and controlled insertion of functional groups on the overall framework. Infrared spectroscopy confirms the presence of the respective functional groups attached to the quaternary carbon atoms at the core of the monomer units, e.g. the band at 1158 cm^{-1} highlights the C-O stretching of the tertiary alcohol while the bands at 3320 and 3380 cm^{-1} indicate the presence of the primary amine group (ESI). The high stability of the frameworks (over 400°C) was demonstrated by TGA analysis.

N_2 adsorption isotherms, collected at 77 K respectively provided Langmuir and BET surface areas of 1565, 1343, 1108 $m^2 g^{-1}$ and 1383, 1190, 984 $m^2 g^{-1}$ for TAF, TAF-NH_2 and TAF-OH (Figure 1). The surface areas and pore-volumes (0.95, 0.68 and 0.45 $cm^3 g^{-1}$ for TAF, TAF-NH_2 and TAF-OH), despite the space occupied by the organic functions in the pores, are outstanding and comparable (or superior) to many of the best performing functionalized POFs.[6] Indeed, there was a considerable contribution of mesoporosity to the total pore volume. N_2 desorption branches run distinctly above the adsorption curves, especially for TAF, forming large hysteresis loops indicative of the framework swellability with an increased pore capacity of more than 40% after expansion. Structure expandability of TAF in the presence of well-interacting 'solvents' was visually observed in the expansion in volume from dry to soaked powder (Figure 1f,g). After filtering the imbibed sample, the increase in weight was evaluated quantitatively to be 370% for acetone, 470% for hexane and 740% for ethylacetate. Unlike the frameworks produced by Friedel-Craft reaction, in which flexibility was introduced by linear connecting chains,[4e,7] we achieved flexible frameworks through the intrinsic connectivity among the monomer units. Indeed, the number of branches protruding from the monomer units is limited to 3 in TAFs, as opposed to 4 in the rigid PAFs,[4a] allowing for a larger conformational adaptability.

Particle size distribution, as determined by Dynamic Light Scattering in dilute suspensions, follow Gaussian profiles centered at 40 nm, with 96% of the particles restricted to the 10-100 nm range, irrespective of the 3 compounds, consistently with the preservation of a constant and homogeneous reaction course even in the presence of diversified functions in the monomer. This nanometric particle size is considered of interest for cell internalization and is thus suitable for drug-delivery.[8]

CO_2 adsorption isotherms recorded at three distinct temperatures (273K, 283K and 298K) revealed excellent uptakes already at low pressure (Figure 2). The uptake up to 1 bar is relevant, reaching 1.9 mmol g^{-1} at ambient temperature and 3.2 mmol g^{-1} at 273 K in TAF-NH_2: these values appear attractive for applications, also considering the relatively low cost of triphenylmethane and its derivatives and the high thermal stability of the frameworks.

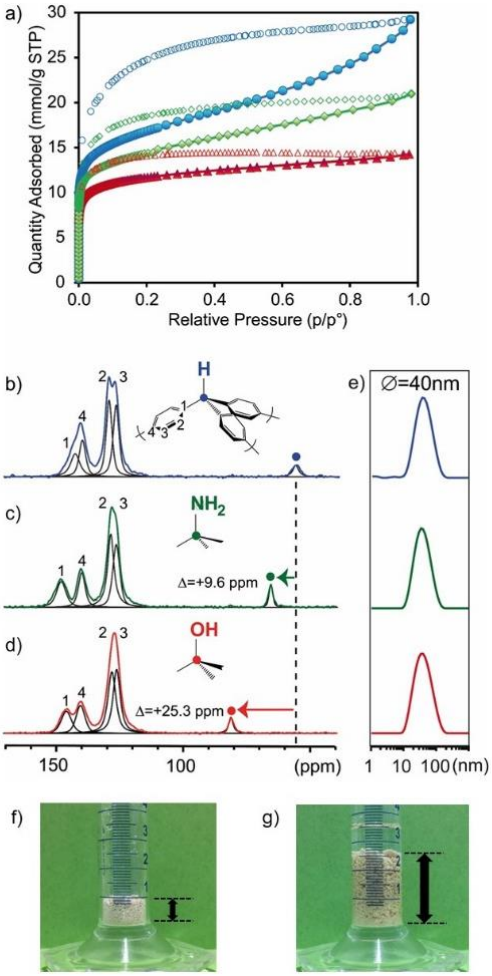

Figure 1. a) N_2 adsorption/desorption isotherms at 77 K of TAF (blue circles), TAF-OH (red triangles) and TAF-NH_2 (green diamonds). ^{13}C MAS NMR spectra of b) TAF, c) TAF- NH_2 and d) TAF-OH. e) Particle size distribution of TAF, TAF-NH_2 and TAF-OH (blue, green and red lines, respectively). f,g) Images of dry and soaked TPAF powder in ethylacetate, respectively.

In general, these are competitive with the best performing porous materials of similar pore capacity, irrespective of the family they belong to: covalent, metal-organic or molecular crystals.[2a,3a,6a] The adsorption isotherms recorded at three distinct temperatures and elaborated by van't Hoff equation, yielded the adsorption energy at low coverage as high as 54 kJ mol^{-1} (13 kcal mol^{-1}) for the amine derivative, which outperforms the other two compounds (26 kJ mol^{-1} and 30 kJ mol^{-1} for TAF and TAF-OH) and is comparable to the highest values of amine-containing POPs.[6a] The strong interaction of TAF-NH_2 was accounted for by the favorable activity of the aliphatic amines. Our choice to exploit aliphatic primary amine as the active component of the framework was successful and confirms their outstanding effectiveness for CO_2 capture and sequestration.

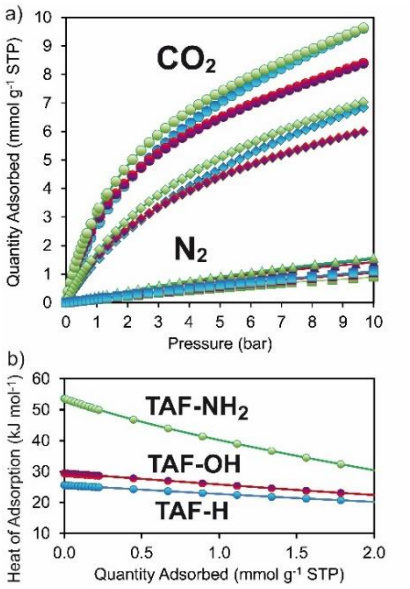

Figure 2. a) CO_2 isotherms of TAF, TAF-NH_2 and TAF-OH (273K: blue, green and red circles; 298 K: blue, green and red diamonds, respectively) and N_2 adsorption isotherms TAF, TAF-NH_2 and TAF-OH (273 K: blue, green and red triangles; 298 K: blue, green and red squares, respectively). b) Isosteric heat of adsorption of TAF-NH_2, TAF-OH and TAF (green, red and blue circles, respectively).

The direct spectroscopic observation of the intimate spatial relationship between the CO_2 gas and the NH_2 groups exposed to the cavity walls in the porous matrix was provided by 2D ^{1}H-^{13}C heterocorrelated MAS NMR (Figure 3). The spectrum recorded at 215 K shows through-space cross-correlations[9] between ^{1}H of the matrix and ^{13}C-enriched CO_2 carbons which are depleted of hydrogens ($\delta(CO_2)$= 125.1 ppm). Thus, CO_2 was found in the slow exchange regime with the interacting sites on the matrix walls, and spent a relatively long time over an individual site, producing an efficient magnetization transfer by dipole-dipole interactions that took place at distances as short as 5-10 Å.[10] In the 2D-heterocorrelated spectrum, NH_2 hydrogens correlate with CO_2 carbons, indicating that the CO_2 molecules sit in close contact with the amine group.[11] Also, the NH_2 interaction site is surrounded by aromatic hydrogens that correlate with CO_2. These results are rare spectroscopic observations, supporting the highly energetic binding of CO_2 in porous materials.[10,12]

The CH_4 adsorption measurements collected up to 10 bar and variable temperature (273, 283 and 298 K) indicate stimulating sorption values (ESI). The binding energies at low coverage exhibit values of 18 and 19 kJ mol^{-1} for TAF and TAF-NH_2, respectively, and up to 21 kJ for TAF-OH (Figure 4). The intermolecular interactions were further increased by the transformation of the -OH group into Li-alkoxide by treatment with lithium hydride in THF. The compound, denonimated TAF-OLi, showed excellent CH_4 binding energy performance, reaching a value as high as 25 kJ mol^{-1} (Figure 4). This quite notable value matches, or even exceeds, the performance of MOFs i.e. Ni-MOF-74 (21.4 kJ mol^{-1}), PCN-14 (18.7 kJ mol^{-1}) and HKUST-1 (17 kJ mol^{-1}).[13a]

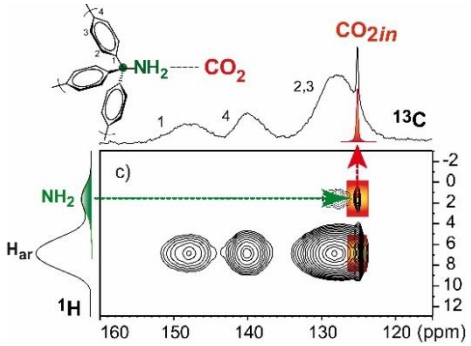

Figure 3. 2D ^{1}H-^{13}C HETCOR MAS NMR spectrum of TAF-NH_2 loaded with ^{13}C-enriched CO_2 at 215K. A contact time of 5 ms was applied. 1D ^{13}C CP MAS NMR spectrum and 1D ^{1}H projection of the sample are reported.

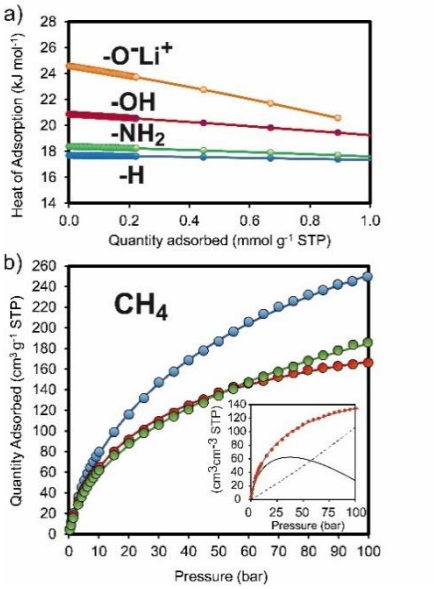

Figure 4. a) CH_4 isosteric heat of adsorption of TAF-OLi, TAF-OH, TAF-NH_2 and TAF (orange, red, green and blue circles, respectively). b) CH_4 adsorption isotherms at room temperature and up to 100 bar of TAF, TAF-NH_2 and TAF-OH (blue, green and red circles, respectively), the value of the total adsorption volume over grams is reported versus pressure. In the inset CH_4 adsorption isotherm of TAF-OH: the value of the total adsorption volume over volume is reported versus pressure. The black line represents the differentce between the total adsorption value and the pure compressed CH_4 while the dashed line the pure compressed CH_4.

Interest in the delivery of large amounts of natural gas has led to the exploration of middle/high pressure solutions in the presence of absorbent materials, thus, methane isotherms of TAFs have been recorded up to 100 bar and room temperature (Figure 4). The volumetric uptake, that is important for Adsorbed Natural Gas Technology (ANG), is shown in Figure 4. The results are encouraging since a total adsorption value of 100 cm^{3}cm^{-3} is achieved at 38 bar with a gain of 64 cm^3 cm^{-3} with respect to compressed methane. This gain is reduced significantly only under extreme conditions. The adsorption values at 35 and 65 bar are of 95 and 119 cm^{3}cm^{-3}, comparable to POPs and exceeding the performance of COF-8, COF-5[13b] and DUT-13, MOF-210 and MOF-200.[13c]

The investigation of porous frameworks generated by branched monomers moved us to the design of 3D aromatic frameworks (TAFs), starting from monomers with three rigid aromatic

branches and a functional group connected to the same tetrahedral core. This arrangement ensures the generation of a robust covalent scaffold, resistant to structural collapse, and with well-anchored organic functions, regularly spaced all over the framework. The newly-designed strategy satisfies the requirements for creating a framework that supports –OH, -NH_2 and –O^-Li^+, which are constantly exposed to the galleries. The frameworks were proved effective in capturing CO_2 and, especially, the amine derivative contains an energetic binding site in each monomer unit accounting for 54 KJ mol^{-1}. The direct spectroscopic observation of CO_2 over the sites was provided by the magnetization transfer from amine hydrogens to CO_2 carbon nuclei through a short-distance dipolar interaction. Methane was a second target gas due to its importance in energy supply, since its transportation can cause concern on both large and small scales. Indeed, the functional materials proposed here, besides the extraordinary chemical and thermal stability, exhibit relevant sorptive properties and excellent capacity, even in high-pressure regimes, owing to the balance between micro- and meso-porosity. From the applicative point of view, it is worthwhile mentioning the relatively low cost of triphenylmethane and derivatives, which constitute the building blocks of the TAF frameworks. Further properties of the present frameworks include network swellability for the creation of functional gels, and the formation of copolymers containing complementary organic groups, to access specialized functions.

Conflicts of interest

There are no conflicts to declare.

Acknowledgements

A.C. would like to thank PRIN 2015, Cariplo Foundation (Balance) and INSTM Consortium/RL for financial supports.

Notes and references

1 E. S. Sanz-Pérez, C. R. Murdock, S. A. Didas and C. W. Jones, *Chem. Rev.*, 2016, **116**, 11840.

2 *(a)* A. Schoedel, Z. Li and O. M. Yaghi, *Nature Energy,* 2016, *1*, 1-13; *(b)* H. C. Zhou and S. Kitagawa, *Chem. Soc. Rev.,* 2014, **43**, 5415-5418; *(c)* K. Sumida, D. L. Rogow, J. A. Mason, T. M. McDonald, E. D. Bloch, Z. R. Herm, T.-H. Bae, and J. R. Long, *Chem. Rev.,* 2012, **112**, 724-781. *(d)* K. Adil, Y. Belmabkhout, R. S. Pillai, A. Cadiau, P. M. Bhatt, A. H. Assen, G. Maurin and M. Eddaoudi, *Chem. Soc. Rev.*, 2017, **46**, 3402-3430.

3 *(a)* J. R. Holst, A. Trewin and A. J. Cooper, *Nature Chem.,* 2010, **2**, 915-920. *(b)* Z. Zhang and M. J. Zaworotko, *Chem. Soc. Rev.,* 2014, **43**, 5444-5455. *(c)* S. Das, P. Heasman, T. Ben and S. Qiu, *Chem. Rev.,* 2017, **117**, 1515-1563. *(d)* V. N. Yadav, A. Comotti, P. Sozzani, S. Bracco, T.-B. Hansen, M. Hennum, and C. H. Gorbitz, *Angew. Chem. Int. Ed.*, 2015, **54**, 15684-15688. *(e)* I. Bassanetti, F. Mezzadri, A. Comotti, P. Sozzani, M. Gennari, G: Calestani, and L. Marchio', *J. Am. Chem. Soc.*, 2012, **134**, 9142-9145. *(f)* S. Galli, A. Maspero, C. Giacobbe, G. Palmisano, L. Nardo, A. Comotti, I. Bassanetti, P. Sozzani, and N. Masciocchi, *J. Mater. Chem. A*, 2014, **2**, 12208-12221. *(g)* A. Comotti, S. Bracco, P. Valsesia, L. Ferretti, and P. Sozzani, *J. Am. Chem. Soc.*, 2007, **129**, 8566-8576. *(h)* P. Sozzani, S: Bracco, A. Comotti, L. Ferretti, and R. Simonutti, *Angew. Chem. Int. Ed.,* 2005, **44**, 1816-1820. *(i)* A. Comotti, S. Bracco, A. Yamamoto, M. Beretta, T. Hirukawa, N. Tohnai, M. Miyata, and P. Sozzani, *J. Am. Chem. Soc*., 2014, **136**, 618-621. *(l)* T. Muller, and S. Bräse, *RSC Advances*, 2014, **4**, 6886-6907.

4 *(a)* T. Ben, H. Ren, S. Ma, D. Cao, J. Lan, X. Jing, W. Wang, J. Xu, F. Deng, J. M. Simmons, S. Qui and G. Zhu, *Angew. Chem. Int. Ed.,* 2009, **48**, 9457-9460. *(b)* W. Lu, D. Yuan, J. Sculley, D. Zhao, R. Krishna, and H.-C. Zhou, *J. Am. Chem. Soc.,* 2011, **133**, 18126-18129. *(c)* W. Lu, J. P. Sculley, D. Yuan, R. Krishna, Z. Wei, and H.-C. Zhou, *Angew. Chem. Int. Ed.*, 2012, **51**, 7480-7484. *(d)* T. Islamoglu, T. Kim, Z. Kahveci, O. M. El-Kadri and H. M. El-Kaderi, *J. Phys. Chem. C*, 2016, **120**, 2592-2599. *(e)* S. Bracco, D. Piga, I. Bassanetti, J. Perego, A. Comotti, and P. Sozzani, *J. Mater. Chem. A*, 2017, **5**, 10328-10337.

5 P. C. Hiemenez, and T. P. Lodge, *Polymer Chemistry*, CRC Press, CRC Press, New York, 2007.

6 *(a)* L. Zou, Y. Sun, S. Che, X. Yang, X. Wang, M. Bosch, Q. Wang, H. Li, M. Smith, S. Yuan, Z. Perry, and H.-C. Zhou, *Adv. Mater.*, 2017, **29**, 1700229. *(b)* S. J. Garibay, M. H. Weston, J. E. Mondloch, Y. J. Colonb, O. K. Fahra, J. T. Hupp, and S. T. Nguyen, *Cryst. Eng. Comm.*, 2013, **15**, 1515–1519. *(c)* M. H. Weston, O. K. Fahra, B. G. Hauser, J. T. Hupp, and S. T. Nguyen, *Chem. Mater.*, 2012, **24**, 1292-1296.

7 *(a)* C. Wilson, M. J. Main, N. J. Cooper, M. E. Briggs, A. I. Cooper and D. J. Adams, *Polym. Chem*., 2017, **8**, 1914-1922. *(b)* K. Ulbrich, K. Hola, V. Subr, A. Bakandritsos, J. Tucek, and R. Zboril, *Chem. Rev.*, 2016, **116**, 5338−5431.

8 Y. Dai, C. Xu, X. Sun, and X. Chen, *Chem. Soc. Rev.*, 2017, **46**, 3830-3852.

9 *(a)* S. Bracco, A. Comotti, L. Ferretti, and P. Sozzani, *J. Am. Chem. Soc.*, 2011, **133**, 8992-8994. *(b)* A. Comotti, S. Bracco, M. Mauri, S. Mottadelli, T. Ben, S. L. Qiu, and P. Sozzani, *Angew. Chem. Int. Ed.*, 2012, **51**, 10136-10140. *(c)* S. Bracco, A. Comotti, P. Valsesia, M. Beretta, and P. Sozzani, *Cryst. Eng. Comm.*, 2010, **12**, 2318-2321. *(d)* K. Kishida, Y. Okumura, Y. Watanabe, M. Mukoyoshi, S. Bracco, A. Comotti, P. Sozzani, S. Horike, and S. Kitagawa, *Angew. Chem. Int. Ed.,* 2016, **55**, 13784-13788.

10 *(a)* A. Comotti, A. Fraccarollo, S. Bracco, M. Beretta, G. Distefano, M. Cossi, L. Marchese, C. Riccardi, and P. Sozzani, *Cryst. Eng. Comm.*, 2013, **15**, 1503-1507. *(b)* S. Brown, *Prog. Nucl. Magn. Reson. Spectrosc.*, 2007, **50**, 199-251. *(c)* S. Bracco, T. Miyano, M. Negroni, I. Bassanetti, L. Marchio', P. Sozzani, N. Tohnai, and A. Comotti, *Chem. Comm.*, 2017, **53**, 7776-7779. *(d)* I. Bassanetti, A. Comotti, P. Sozzani, S. Bracco, G. Calestani, F. Mezzadri, and L. Marchio', *J. Am. Chem. Soc.*, 2014, **136**, 14883-14895. *(d)* S. Bracco, F. Castiglioni, A. Comotti, S. Galli, M. Negroni, A. Maspero, and P. Sozzani, *Chem. Eur. J.*, 2017, **23**, 11210-11215.

11 R. Vaidhyanathan, S. S. Iremonger, G. K. Shimizu, P. G. Boyd, S. Alavi, and T. K. Woo, *Science*, 2010, **330**, 650-653.

12 *(a)* M. McDonald, et al., *Nature*, 2015, **519**, 303-308.

13 *(a)* Y. Penag, V. Krungleviciute, I. Eryazici, J. T. Hupp, O. K. Farha and T. Yildirim, *J. Am. Chem. Soc.*, 2013, **135**, 11887-11894. *(b)* B. Li, H.-M. Wen, W. Zhou, J. Q. Xu and B. Chen, *Chem.*, 2016, **1**, 557-580. *(c)* J. A. Mason, M. Veenstra and J. R. Long, *Chem. Sci.*, 2014, **5**, 32-51.

